PHILOSOPHICAL TRANSACTIONS A

rsta.royalsocietypublishing.org

Research

Cite this article: Jerosch K, Pehlke H, Monien P, Scharf F, Weber L, Kuhn G, Braun MH, Abele D. 2018 Benthic meltwater fjord habitats formed by rapid glacier recession on King George Island, Antarctica. *Phil. Trans. R. Soc. A* **376**: 20170178.
http://dx.doi.org/10.1098/rsta.2017.0178

Accepted: 29 January 2018

One contribution of 14 to a theme issue 'The marine system of the West Antarctic Peninsula: status and strategy for progress in a region of rapid change'.

Subject Areas:
pattern recognition, geochemistry, hydrology, oceanography

Keywords:
glacial discharge, radius of impact, *k*-means cluster analysis, meltwater fjord habitats, West Antarctic Peninsula

Author for correspondence:
Kerstin Jerosch
e-mail: kerstin.jerosch@awi.de

†Present address: Functional Ecology, Alfred Wegener Institute, Helmholtz Centre for Polar and Marine Research, Am Handelshafen 12, 27570 Bremerhaven, Germany.

Electronic supplementary material is available online at https://doi.org/10.6084/m9.figshare.c.4064252.

THE ROYAL SOCIETY PUBLISHING

Benthic meltwater fjord habitats formed by rapid glacier recession on King George Island, Antarctica

Kerstin Jerosch[1,2,†], Hendrik Pehlke[1,2], Patrick Monien[3,4], Frauke Scharf[1], Lukas Weber[5], Gerhard Kuhn[1], Matthias H. Braun[6] and Doris Abele[1]

[1]Bio- and Geosciences Divisions, Alfred Wegener Institute, Helmholtz Centre for Polar and Marine Research, Am Handelshafen 12, 27570 Bremerhaven, Germany
[2]Helmholtz Institute for Functional Marine Biodiversity, and
[3]Institute for Chemistry and Biology of the Marine Environment (ICBM), University of Oldenburg, Carl-von-Ossietzky-Strasse 9-11, 26129 Oldenburg, Germany
[4]Faculty of Geosciences, University of Bremen, Klagenfurter Strasse 2-4, 28359 Bremen, Germany
[5]Information Management and Media, Karlsruhe University of Applied Sciences, Moltkestraße 30, 76133 Karlsruhe, Germany
[6]Institute for Geography, Friedrich-Alexander-Universität Erlangen-Nürnberg, Wetterkreuz 15, 91058 Erlangen, Germany

KJ, 0000-0003-0728-2154

The coasts of the West Antarctic Peninsula are strongly influenced by glacier meltwater discharge. The spatial structure and biogeochemical composition of inshore habitats are shaped by large quantities of terrigenous particulate material deposited in the vicinity of the coast, which impacts the pelagic and benthic ecosystems. We used a multitude of geochemical and environmental variables to identify the radius extension of the meltwater impact from the Fourcade Glacier into the fjord system of Potter Cove, King George Island. The *k*-means cluster algorithm, canonical correspondence analysis, variance analysis and Tukey's post hoc multiple comparison tests were applied to define and cluster coastal meltwater habitats. A minimum of 10 clusters were needed to classify the 8 km^2 study area into meltwater fjord habitats (MFHs), fjord habitats and marine habitats.

Strontium content in surface sediments is the main geochemical indicator for lithogenic creek discharge in Potter Cove. Furthermore, bathymetry, glacier distance and geomorphic positioning are the essential habitats explaining variables. The mean and maximum MFH extent amounted to 1 km and 2 km, respectively. Extrapolation of the identified meltwater impact ranges to King George Island coastlines, which are presently ice-covered bays and fjord areas, indicated an overall coverage of 200–400 km^2 MFH, underpinning the importance of better understanding the biology and biogeochemistry in terrestrial marine transition zones.

This article is part of the theme issue 'The marine system of the West Antarctic Peninsula: status and strategy for progress in a region of rapid change'.

1. Introduction

If greenhouse gas atmospheric concentrations continue to increase at the present rate, temperatures across the Antarctic continent are projected to increase by several degrees and sea ice will be reduced by about one-third [1]. Rising air temperatures and upwelling of warm circumpolar deep waters cause thinning and loss of sea ice and a rapid retreat of tidewater glaciers that discharge into the warm surface waters in the southwestern Antarctic Peninsula region [2]. Within the northern section of the western Antarctic Peninsula (WAP), including Bransfield Strait where ocean surface temperatures are cooler, only about 50% of the glaciers are on the retreat, and frontline changes are less pronounced than further south [3]. The ice caps and tributary glaciers of the South Shetland Islands in the western Bransfield Strait (figure 1) show rapid surface melting under the influence of warm and moist air intrusions from South America as a consequence of more frequent positive Southern Annual Mode phases [4,5]. On King George Island (KGI), the largest of the South Shetland Islands, most of the glaciers that discharge into fjords and the coastal ocean are retreating at an unprecedented speed [6]. As a result of glacier frontline retreat along the scattered KGI coastline (457 km) newly ice-free areas are exposed to the effects of thawing of permafrost, ice masses and erosion on land. According to the analysis carried out by Rückamp *et al*. [7], around 44% of the coast was ice free in 2008. In marine coastal areas, rising water temperature, turbidity, fast ice timing, ice disturbance and chemical factors, including nutrient and carbon biogeochemistry and meltwater discharge from the ice cap, alter the abiotic living conditions in densely colonized benthic habitats. Collectively, these changing factors and processes influence the bloom dynamics of primary producers and trigger cascading effects throughout the food web [8–11]. The distribution of benthic fauna is controlled by a combination of biological and environmental factors. Many species show a particular affinity for certain types of substrate, which provide a physical habitat or structure that is directly or indirectly suited for their mode of living [12–18]. Alteration of the habitat availability changes community structure as species start to expand their habitat and compete on newly opening spaces [19,20], or compete for the limited remaining space they want to occupy in sediment-impacted zones.

The effects of climate-induced glacier retreat on the biological structures and the functioning of Antarctic fjord ecosystems are the focus of multi-national research programmes currently investigating WAP climate change effects. A major focus of the research at the Argentinian/German Dallmann Laboratory (Carlini Station, Potter Cove, KGI) is to investigate the influence of the fast retreat of the Fourcade Glacier, which has been exclusively land based since 2016 [21], on benthic ecosystems. The glacier's retreat has strongly altered the fjord ecosystem structure and functioning and will continue to do so while it continues to retreat on land. A long-term air temperature and hydrographic data series has been running since 1991 [22], accompanying the observations of environmental and ecological change in this area. An important driver of change is the discharge of suspended particulate matter (SPM) from below the glacier and from thawing permafrost (and soils) on land into Potter Cove [23]. The SPM limits light availability, particularly during the summer melt season, and causes increased sediment accumulation on the sea floor close to the glacier. In coastal areas such as Potter Cove, the

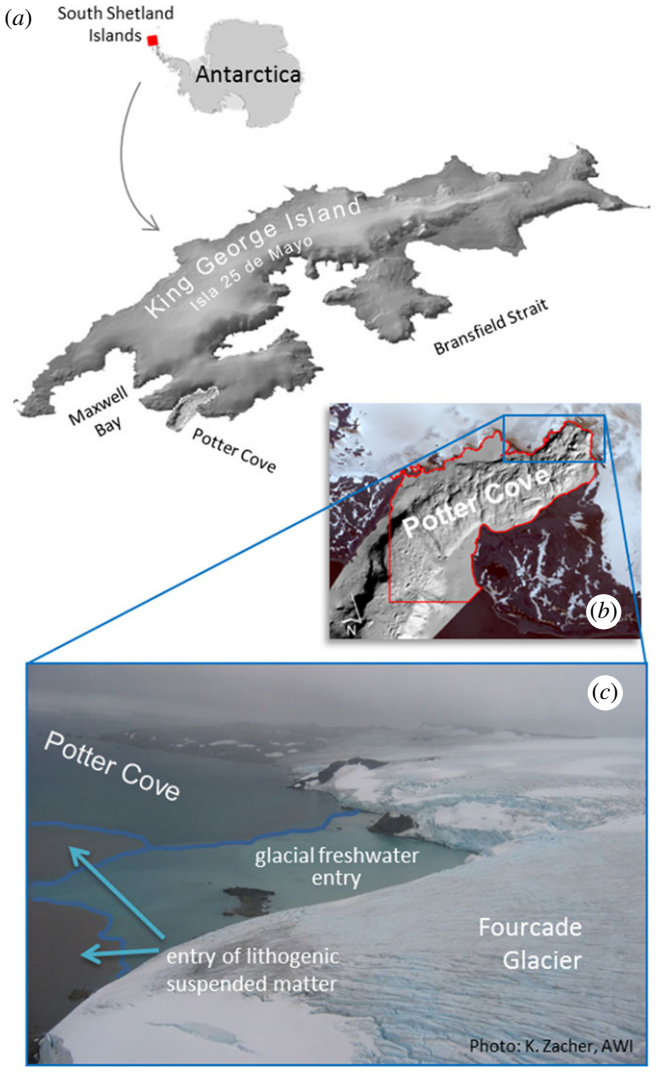

Figure 1. Potter Cove at King George Island/Isla 25 de Mayo, West Antarctic Peninsula (*a*). The red polygon in (*b*) highlights the extent of the study area. Meltwater and lithogenic suspended matter entry from Fourcade Glacier into Potter Cove is indicated in (*c*).

meltwater that discharges as groundwater from land to sea [24] also shapes the geochemistry of the soft sediments [25,26] with consequences for the redox state, solubility and bioavailability of important micronutrients in pore waters [25,26]. The immediate ecological effects of this sediment release comprise impacts on the local biodiversity [27,28], animal energetics and growth rates [14,29,30] and on benthic community composition and community distribution [27,31,32] within the cove.

The scarcity of complete and consistent datasets in West Antarctic coastal areas that cover all ecosystem compartments from the cryosphere to the ocean, the sediments and the biology in sufficient temporal and spatial resolution hampers a clear understanding of the severity of the ongoing climate-induced coastal change processes. Data analysts are often confronted with heterogeneous, uneven and sparsely distributed datasets, or with insufficient temporal resolution of highly varying parameters. Significant resolution is only obtained in long-lasting observations; and many datasets are limited to the summer seasons. Given these restrictions, it is often a major challenge to apply robust statistical methods to the available datasets, to provide measures for

uncertainties and to define larger areas valid for extrapolation of the knowledge acquired from small-scale investigations.

In the present study, we used a comprehensive data pool of 42 abiotic variables available for Potter Cove, an 8 km^2 fjord system, to distinguish meltwater fjord habitats (MFHs) from fjordic habitats (FHs) and marine habitats (MHs). Habitats and sub-habitats or 'clusters' are useful spatial categories to enable the quantification of biogeochemical processes (e.g. micronutrient budgets and turnover rates) under the impact of spatially heterogeneous patterns of glacier retreat and meltwater discharge. Furthermore, such spatial units can be used for the extrapolation of species abundance and habitat studies to larger areas in support of the optimization of future benthic surveys and sampling strategies.

The aim of our study was to determine the radius of glacial meltwater impact on the benthic fjord ecosystems in Potter Cove. Based on the set of environmental variables, the habitats of the fjord are structured for a representative differentiation between benthic MFHs, non-influenced benthic FHs and MHs adjacent to the fjord. Based on the MFH distance to Fourcade Glacier, a first approximation of the KGI coastal areas that are most likely affected by meltwater can be done.

2. Material and methods

(a) Study area

The South Shetland Islands are a 550 km long mostly ice-capped archipelago located at the northern tip of the Antarctic Peninsula. KGI (62°23′ S, 58°23′ W) is the largest of the South Shetland Islands, located 130 km from the northwestern tip of the Antarctic Peninsula. Its 1250 km^2 ice cap reaches a maximum elevation of around 720 m.a.s.l. [6]. Potter Cove is an approximately 8 km^2 small inlet opening into Maxwell Bay (figure 1*a*), which is a large fjord system located between KGI and Nelson Island. Fourcade Glacier descends from the Warzawa Ice Field and drains from the northeast into the head of the cove. The tidewater glacier tongue retreated at a mean rate of 20 m a^{-1} between 1956 and 2008 [7] and has been entirely land based since 2016 [21]. The north-eastern coast is confined by ice cliffs, whereas gravel beach ridges intersected by meltwater streams occupy the southern coast [33]. Moraines, moraine incisions and glacial lineations on the sea floor in the inner part of the cove and pockmarks, ice scour marks and channel structures in the outer part reveal glacial recessions, still stands and potential re-advances during the Late Holocene [34]. The first moraine separates the outer from the inner cove area. The study area (red polygon in figure 1*b*) was defined by the distribution of available data and covers the entire inner cove area (5.21 km^2) and approx. 1.95 km^2 of the outer cove. Meltwater and lithogenic suspended matter entry from Fourcade Glacier into Potter Cove is indicated in figure 1*c*.

(b) Environmental data

The analysis accounted for 42 environmental variables assessed mainly at or close to the sea floor. The majority of the data result from sediment cores taken during the Austral summer seasons 2010/2011 and 2011/2012 (https://doi.pangaea.de/10.1594/PANGAEA.832335 https://doi.pangaea.de/10.1594/PANGAEA.815205 and https://doi.pangaea.de/10.1594/PANGAEA.853593). For sample preparations and geochemical analyses refer to Monien *et al*. [25]; for grainsize analysis refer to [35]. The entire sampling period includes the years 1992–2015. Data and data sources are listed in table 1; the electronic supplementary material, appendix S1, figure S1, contains the plots of the processed raster data projected in UTM21 coordinates, which are made accessible from the data archive Pangaea (https://doi.pangaea.de/10.1594/PANGAEA.856971). The geochemical and sediment texture raster data result from the interpolation of the upper part of the sediment cores (first 5 cm) by using the Geostatistical Analyst ArcGIS 10.4.1 (ESRI). On this occasion, the statistical mean values (e.g. s.e.m., standardized root mean square error and

Table 1. Variables included in the *k*-means cluster analysis in alphabetic order. Geochemical and sediment texture data relate to the first 5 cm of sediment short core data (surface). The Sr and TOC mean over the total core (min 0.5 cm; max 44.5 cm) were also included (mean). The BPI provides an indication of the geomorphic features such as depressions or slopes [36]. Processed data are downloadable as 5 m × 5 m raster datasets (https://doi.pangaea.de/10.1594/PANGAEA.856971) and are presented in the electronic supplementary material, appendix S1; figure S1.

parameter	source	parameter	source
aluminium oxide (wt%), Al_2O_3, surface	[25]	sodium oxide (wt%), Na_2O, surface	[25]
barium (mg kg^{-1}), Ba, surface	[25]	nickel (mg kg^{-1}), Ni, surface	[25]
bathymetry (m)	[37]	rubidium (mg kg^{-1}), Rb, surface	[25]
bed shear stress (N m^{-2})	[38]	sand (%), surface	[35]
benthic positioning index, BPI, broad	this study	satellite image (SPM remote)	DigitalGlobe, Inc.[a]
benthic positioning index, BPI, fine	this study	silt (%), surface	[35]
calcium oxide (wt%), CaO, surface	[25]	silicon dioxide (wt%), SiO_2, surface	[25]
clay (%), surface	[35]	slope (°)	this study
cobalt (mg kg^{-1}), Co, surface	[25]	susp. particulate matter (mg l^{-1}), SPM, surface	[23]
chromium (mg kg^{-1}), Cr, surface	[25]	strontium (mg kg^{-1}), Sr, mean	[25]
copper (mg kg^{-1}), Cu, surface	[25]	strontium (mg kg^{-1}), Sr, surface	[25]
distance to coast (m)	this study	titanium oxide (wt%), TiO_2, surface	[25]
distance to glacier (m)	this study	total organic carbon (%), TOC, mean	[25]
iron oxide (wt%), Fe_2O_3, surface	[25]	total organic carbon (%), TOC, surface	[25]
hard substrate probability (%)	[35]	total sulfur (wt%), TS, surface	[25]
lead (mg kg^{-1}), Pb, surface	[25]	velocity (m s^{-1}), bottom currents, mean	[38]
phosphorus oxide (wt%), P_2O_5, surface	[23,25]	velocity (m s^{-1}), bottom currents, max	[38]
potassium oxide (wt%), K_2O, surface	[25]	velocity, (m s^{-1}), surface currents, mean	[38]
magnesium oxide (wt%), MgO, surface	[25]	yttrium (mg kg^{-1}), Y, surface	[25]
manganese oxide (wt%), MnO, surface	[25]	zinc (mg kg^{-1}), Zn, surface	[25]
mud (wt%), surface	[35]	zirconium (mg kg^{-1}), Zr, surface	[25]

[a] © [2013] DigitalGlobe, Inc., provided by European Space Imaging.

averaged standard error) resulting from different interpolation methods (e.g. inverse distance weighted, Indicator, Bayesian, Ordinary and Co-Kriging) and iteratively changing settings (e.g. lag size, range, neighbour type, anisotropy) have been evaluated to decide on the raster dataset used for further analysis (electronic supplementary material, appendix S1; table S1). The bathymetry served to generate more detailed information about the benthic environment by slope and the benthic positioning index (BPI) [36,39]. The BPI is a measure of site depth relative to the mean depth of a defined surrounding area (e.g. [40]). For this study, a fine BPI surrounding radius was defined as 0–15 m, and a broad BPI as 15–250 m. The BPI values are positive for depressions, negative for ridges and valleys, and near or equal to zero for constant slopes and flat areas.

(c) Habitat identification by *k*-means clustering

Owing to the large number of objects (here: raster cells) that needed to be clustered, the non-hierarchical clustering method *k*-means was applied in R version 2.2.2 [41]. For the full list of packages used and for citations refer to the electronic supplementary material, appendix S1, tables S4 and S5. *k*-means requires the in-advance specification of the overall number of clusters to be

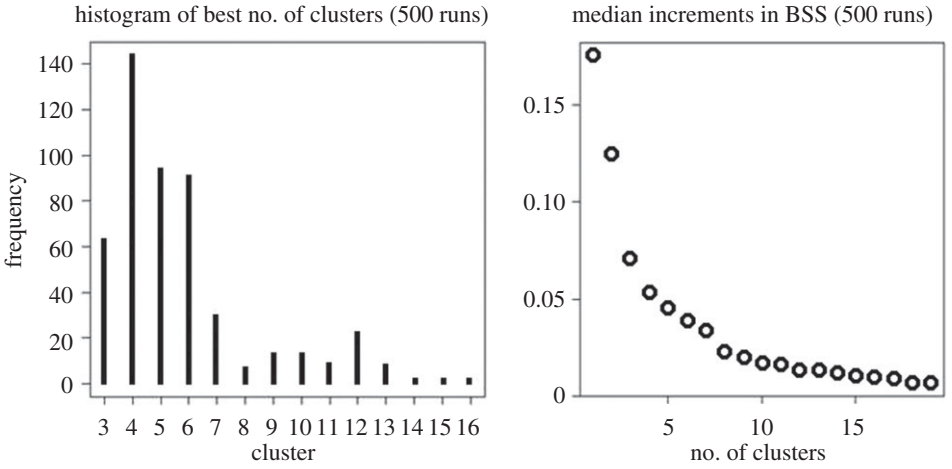

Figure 2. Examination of the optimum cluster numbers for *k*-means clustering application by means of the BSS, which is an index of cluster validity developed by Zhao & Fränti [46].

detected. By either randomly choosing or defining the first set of cluster centres, the *k*-means algorithm assigns all objects to one of these centres. This aims at minimizing the internal multivariate cluster dissimilarity. The resulting cluster means are then calculated and the clusters are recalculated in the same way. This is done as many times as needed to reach a given iteration goal (e.g. no differences between cluster centres). In this way, optimal internal homogeneity is achieved in the resulting groups [42,43].

The ideal determination of *k* will balance between the maximum compression of the data using a single cluster and the maximum accuracy by assigning each datum point to its own cluster. Different types of optimization criteria to calculate clusters with a minimized total intra-cluster variation are available, such as the within-cluster sum of squares, the Akaike information criterion (AIC) or the Bayesian information criterion (BIC) (or total within-cluster sum of squares (WSS)). The total WSS measures the compactness of the clustering and should be as small as possible. A corresponding method to identify the optimum number of clusters called the 'elbow method' plots the WWS according to the number of clusters *k*. The location of a bend (a so-called 'elbow') in the curve is considered to be an indicator of the appropriate number of clusters. Furthermore, a number of statistical testing methods consist in comparing evidence against the null hypothesis (e.g. gap statistics).

Because of the existence of a multitude of indices, 23 different methods were applied in this study and their results were compared to determine the optimum number of clusters. The R package NbClust [44] was used to apply 21 indices and to propose the best clustering scheme from the different results; this was obtained by varying all combinations of numbers of clusters, distance measures and clustering methods. Additionally, the gap statistic method proposed by Tibshirani *et al*. [45] and applied with the R function 'ClusGap' (R package 'cluster') was used to calculate a measure of the goodness of clustering by comparing the total intra-cluster variation for different values of *k* with their expected values under a null reference distribution of the data, i.e. a distribution with no obvious clustering. The method *X-means* refines cluster assignments by repeatedly attempting subdivision and keeping the best resulting splits until a criterion such as the AIC or the BIC is reached. Moreover, the between-cluster sum of squares (BSS) is an index of cluster validity developed by Zhao & Fränti [46] that is a function of the median increments in the BSS (500 runs) and the number of clusters. The first local maximum described the point where the BSS was no longer increasing, indicating the optimal number of clusters.

The results of the different methods applied give no definite answer and recommend different optimum cluster numbers. As an example, the result of the BSS is given in figure 2 and suggests an optimum number of 4 or 12 clusters by visual inspection, and optionally 10. To reduce subjectivity

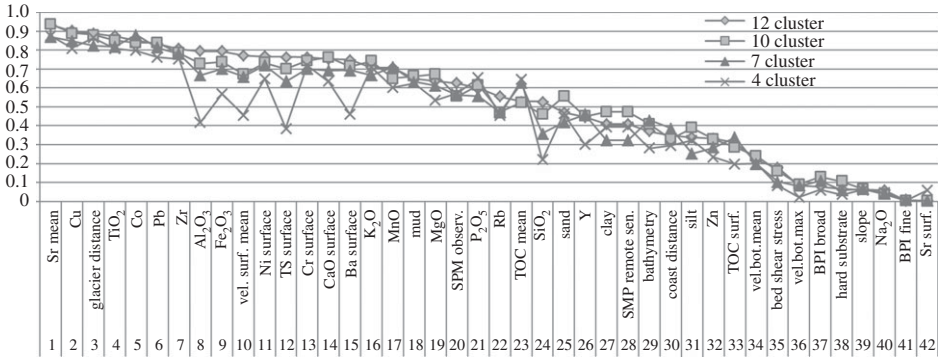

Figure 3. Order of the 42 environmental variables influencing four suggested classification options. The variable order of the four cluster options differs significantly from the alternative option ones.

in decision-making the four most frequently chosen clusters over all indices (4, 7, 10 and 12) were used for further *k*-means clustering.

The entire dataset was kept for further analysis. A Spearman correlation matrix over the 42 variables revealed a higher intercorrelation than 0.9 for only 16 of the 840 analysis pairs (electronic supplementary material, appendix S2) that could cause a bias in the respective cluster result. Five of these correlations concern soil fraction variables and can be explained by compositional data (data describing relative quantities which sum to 100%) [47]. More sand necessarily means less silt and clay. However, all particle size fractions are ecologically relevant and should be kept in the analysis. If a statistical method suggests deleting a variable, preference should be given to ecological and geochemical variables because we do not yet know which of the predictors are important. Omitting a variable may result in a significantly different clustering and is highly affected by pre-selection of variables [48]. Furthermore, large sample sizes ($n \geq 10\,000$, this study $n = 287\,387$) are less prone to bias [49], and the correlation coefficient itself can miss important information such as the level or intensity of difference.

Each of the 42 environmental variables influences the habitat location and extent to a different degree. The curves in figure 3 visualize their order of importance for the four suggested options. According to its curve, the four-cluster option substantially deviates from the alternative options, which is evident from the variable Al_2O_3 onwards (position 8 in the ranking). The deviation was interpreted as a too intense compression of the data; as a consequence, the four-cluster option was excluded from further analysis.

(d) Habitat distinctions

The combination of canonical correlation analysis (CCA) and variance analysis (ANOVA), both implemented in the R package 'vegan', as well as Tukey's post hoc multiple comparison testing (Tukey's honest significant difference (HSD) test; R package 'agricolae') was applied to explain statistically significant differences between habitats in Potter Cove and to identify the influencing factors based on the variables involved.

CCA is a multi-variate method initially used to elucidate the relationships between species assemblages and their environment. Here, we applied CCA exclusively to environmental datasets, thereby benefiting from the specific design of the method that allows synthetic environmental gradients be extracted from ecological datasets. The gradients are the basis for succinctly describing and visualizing the differential characteristics of habitats in an ordination diagram. In short, CCA is based on Chi-squared distances and performs weighted linear mapping. CCA, first introduced by Hotelling [50], is applied here to test whether some variables explain habitat distribution better than others. CCA identifies correlations in an

ordination system based on χ^2-distances and finds linear combinations of two random vectors X_i and Y_j which have maximum correlation with each other [51,52]. CCA was applied to 10 000 subsamples (out of a total of 286 010 raster cells). Subsampling considered the original distribution of sampling across clusters and included 999 permutations per subsample. The differences between the habitats were tested by ANOVA statistics: for each variable and each habitat, a mean value was calculated and compared with the mean value for each habitat. Significant differences between the mean values comparing the habitats were determined by *t*-tests to see whether at least two means were significantly different from each other. Additionally, Tukey's HSD test was applied to test for specific habitat differences. Tukey's HSD test compares all possible pairs of means, and identifies any differences between two means that are greater than the expected standard error. It creates confidence intervals for all pairwise differences of habitats while controlling the mean error rate at the specified significance level ($\alpha = 0.05$).

3. Results

(a) Clustering of meltwater fjord habitats, fjord habitats and marine-influenced habitats

For Potter Cove 4, 7, 10 and 12 clusters were suggested by direct and statistical testing methods for a *k*-means clustering of 42 abiotic variables (figure 2*c*). When applying *k*-means clustering by means of the R package 'cluster', the optimal number of clusters is to a certain extent subjective and depends on the methods used to determine similarities and on the parameters used for cluster partitioning. Validating the clusters with respect to the overall question (in our case: how to best cluster different habitats under melt impact) is therefore essential. The four-cluster option was rejected based on the results from the CCA (figure 3), which showed a divergent order of importance of influencing environmental variables for this option compared with a concordant order of importance for the three remaining options. This deviation was interpreted as inaccuracy resulting from too coarse generalization of the variables (figure 2*c*). The environmental input raster data as well as the results of the three classification options are available from the data archive Pangaea (https://doi.pangaea.de/10.1594/PANGAEA.856971). A summary of area coverage, depth and distance to the glacier per habitat is given in table 2.

Visual inspection of the 7-, 10- and 12-cluster options (figure 4*a–c*) revealed spatial differences between the 7- and 10- (and 12-, respectively) cluster options but no significant difference between the 10- and 12-cluster options in the outer part of the cove. Enclosing habitats H1–H5 (10-cluster option) and H1–H7 (12-cluster option) covers almost the same benthic area in the inner cove (figure 4*d*). This indicates that a minimum of 10 clusters is required to identify the maximum extent of the Fourcade Glacier meltwater influence. The 10-cluster option was hence identified as the optimum number of clusters for the analysis of meltwater-influenced habitats in Potter Cove.

The comparison of the three options further revealed absolutely no spatial change in the area beyond moraine M1 (figure 4*b*) in the outer cove (clusters with the highest number for each option (H7, H10 and H12, figure 4*a–c*)). Therefore, this area was determined as meltwater-unaffected MH. Likewise, unaffected FHs can be distinguished from MFHs through observing similarities between the results of the 10- and the 12-cluster options. The four habitats H6–H9 (10-cluster option) and H8–H11 (12-cluster option) are congruent with each other; neither the area nor the number of clusters changes. These habitats are combined and defined to be the FH. Exclusively, the area across the red line in figure 4*b,c* is broken down into more detail with increasing numbers of clusters and therefore is specified as the MFH. The MFHs derived from the 10-cluster option cover about two-thirds of the investigated Potter Cove area, amounting to 3.18 km^2 (figure 4*d*), with a maximum, minimum and mean water depth of 54.8 m, 0 m and 17.7 m and a maximum, minimum and mean distance to Fourcade Glacier of 2269 m, 0 m and 1033 m, respectively.

Table 2. Area, depth and glacier distance characteristics for all cluster options assigned to MFH, FH and MH.

			depth (m)			glacier distance (m)		
7 habitats		area (km^2)	min	max	mean	min	max	mean
MFH	1	1.0458	−55	0	−24	0	978	381
	2	1.4148	−53	0	−29	615	2451	1559
	3	0.5742	−36	0	−8	849	2250	1528
FH	4	0.8724	−41	0	−10	434	3757	2570
	5	1.2425	−89	0	−35	1194	3925	2815
	6	1.0904	−157	−48	−111	3314	4437	3797
MH	7	0.9103	−73	0	−13	2305	3748	3070
			depth (m)			distance to glacier (m)		
10 habitats		area (km^2)	min	max	mean	min	max	mean
MFH	1	0.2261	−40	0	−8	0	978	223
	2	0.8176	−55	0	−28	0	983	425
	3	0.581	−37	0	−8	849	2267	1532
	4	1.0656	−48	0	−31	619	2269	1488
	5	0.4907	−36	0	−12	445	2205	1497
FH	6	0.6857	−41	0	−10	2058	3701	2837
	7	0.7419	−56	−15	−38	1956	3267	2666
	8	0.6973	−101	0	−35	2177	3941	3136
	9	1.0247	−157	−62	−113	3369	4437	3820
MH	10	0.8198	−73	0	−11	2314	3747	3078
			depth (m)			distance to glacier (m)		
12 habitats		area (km^2)	min	max	mean	min	max	mean
MFH	1	0.2113	−40	0	−8	0	978	226
	2	0.4945	−55	0	−26	0	682	260
	3	0.4837	−51	0	−29	176	1167	735
	4	0.497	−37	0	−13	445	2205	1505
	5	0.7141	−48	−7	−34	919	2216	1591
	6	0.378	−43	0	−24	679	2421	1621
	7	0.4302	−30	0	−4	887	2100	1497
FH	8	0.6805	−41	0	−10	2018	3685	2831
	9	0.7223	−56	−15	−39	1973	3267	2684
	10	0.6943	−101	0	−35	2177	3938	3138
	11	1.026	−157	−62	−113	3369	4437	3819
MH	12	0.8184	−73	0	−11	2316	3747	3079

(b) Abiotic distinctions between meltwater fjord habitats, fjord habitats and marine-influenced habitats

Descriptive statistical measures over all abiotic variables within groups were calculated to characterize the difference between MFHs near the Fourcade Glacier, meltwater-unaffected FHs

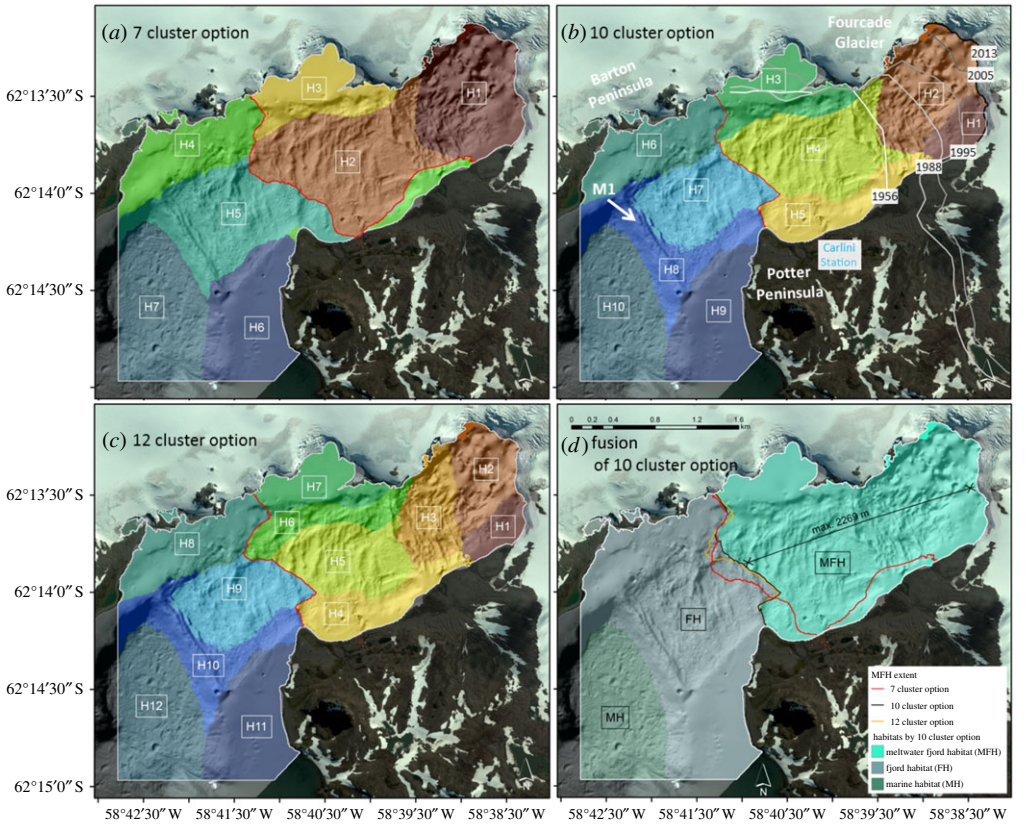

Figure 4. Fjord habitats in Potter Cove resulting from *k*-means cluster analysis of 42 environmental variables realized for 7 (*a*), 10 (*b*) and 12 (*c*) predetermined clusters. The glacier front lines are labelled by years [7]. Extent of meltwater fjord habitats (MFH), fjord habitats (FH) and marine habitats (MH) in Potter Cove based on the preclassification of 10 clusters (*d*). The overlay of the three alternative MFHs (red, black and red lines) reveals a high match between the 10- and 12-cluster options.

and MHs under higher impact in the outer cove. Selected influencing variables enable statistical differentiation of the habitat characteristics. The habitat-conditional triplot based on a CCA in figure 5 simultaneously visualizes habitats and variables. The CCA eigenvector analysis (axes 1 and 2, figure 5*a*) explains 90.0% of the variance (a combination of the inertia in the magnitude and variance in the weighted averages). The ordination diagram summarizes the main correlation structure between the three habitats (MFH, FH and MH) with respect to the 10 most important variables (figure 5*a*) and all 42 environmental variables (figure 5*b*). Quantitative environmental variables are displayed by their correlations with the axes, and qualitative environmental variables by the centroids of the habitats. The CCA plots (figure 5*a*,*b*) and table 3 show that MFH seems to be associated with low levels of Sr (mg kg^{-1}) and CaO (wt%) as well as high contents of CuO (mg kg^{-1}), K_2O (wt%) and clay (%) in surface sediments, high SPM contents in the water column and a shallow water depth (mean −22 m). The mean glacier distance is 1134 m. An FH is positively correlated with CaO (wt%), Sr (mg kg^{-1}), larger glacier distance (mean 2930 m) and also a shallow water depth (mean −24 m). Both types of fjord habitats (MFH and FH) are characterized by positive BPI resulting from glacial excavations. MH is especially characterized by deeper water depth (greater than 112 m). For the full list of statistical mean values of environmental variables comparing MFH, FH and MH refer to the electronic supplementary material, appendix S1, table S2.

Further ANOVA showed that the full model is statistically significant ($p < 0.001$) and the Tukey HSD test revealed that the environmental variables are significantly different in all three habitat

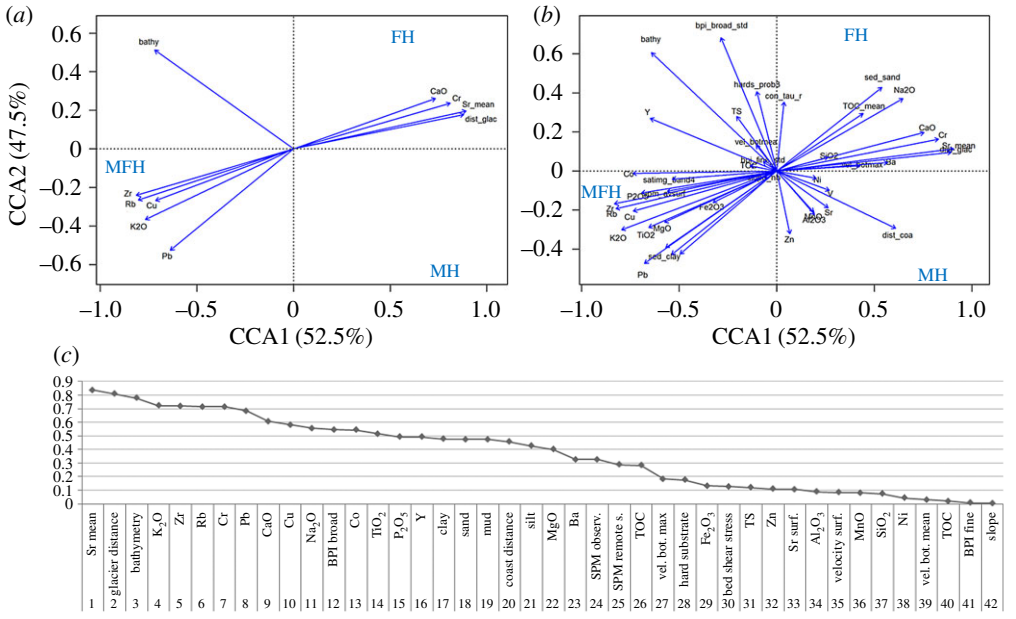

Figure 5. Habitat-conditional triplot for the 10 most important (*a*) and all (*b*) variables based on a CCA displaying inertia (i.e. weighted variance) in the abundances and variance in the weighted averages of 10 000 subsamples ($n_{total} = 286\,010$) with respect to the environmental variables. Quantitative environmental variables are indicated by arrows. The scale marks along the axes apply to the quantitative environmental variables. Importance of influence (*c*) ordered for the classification between MFH, FH and MH.

types (boxplots assigned to different letters in figure 6). The blue letters in figure 6 indicate the degree of similarity between the habitats. A considerable variance effect is visible in the content and concentrations of geochemical elements such as Na, K, Ca of MFH and FH in surface sediments compared with MH. The environment of MFH clearly distinguishes from FH and MH; for instance the contents of Sr and sand in surficial sediments are significantly lower in MFH than in FH or in MH, while mean values of K_2O and clay contents are considerably higher. For comparisons between further statistical mean values of MH, FH and MFH, the full details of all the variables are available in the electronic supplementary material, appendix S1, table S2. Clearly, the CCA applied in this paper to environmental data provided useful habitat knowledge by guaranteeing a maximum dispersion of the weighted variance and variable centroids. Tukey's HSD revealed which habitats are more alike according to the variables (figure 6) and therefore provided additional insight into the ecological differentiation of the habitats. Distinct bathymetry differences occur between MFH and MH (assigned to letters a and c, figure 6), whereas the main differences regarding clay exist between MFH and FH. The mean values for bathymetry and Al_2O_3 clearly separate MH from FH and from MFH.

The determination of MFH in Potter Cove is strongly related to the geochemical properties of the terrestrial sediments and soils originating from the Barton and Potter Peninsulas [53], the glacier distance and the bathymetry (figure 5*c*). Furthermore, the seabed morphology (represented by the broad BPI) and sediment texture (e.g. clay or sand) correlate with the sedimentation processes and are therefore positioned in the upper part of the ranking list.

4. Discussion

Inshore ecosystems at the WAP area are currently changing at an unprecedented speed owing to the rapid melting of coastal glaciers and ice caps. Notwithstanding the overall climatic trends in

Table 3. Selected characteristics describing the benthic habitats and sub-habitats at Potter Cove. MFH, marine fjord habitat; FH, fjord habitat; MH, marine habitat; H, habitat; SubH, sub-habitat; mGlDi, mean glacier distance (m); mBathy, mean bathymetry (m); SPM, suspended particulate matter.

habitats		characteristics										
H	SubH	mGlDi	mBathy	SPM	clay	Sr (mg kg^{-1})	Zr (mg kg^{-1})	Rb (mg kg^{-1})	Cu (mg kg^{-1})	CaO (wt%)	K_2O (wt%)	benthic communities in Potter Cove
MFH	H1	222.5	−7.8	19.6	0.2	331.6	156.6	42.1	109.5	4.5	1.5	filter feeders domination Pennatulacea, Ascidiacea, Ophiuroidea, Asteroidea
	H2	424.2	−28.5	10.0	0.3	329.2	163.0	49.7	113.7	4.1	1.7	
	H3	1531.6	−8.4	3.4	0.2	364.5	167.2	43.5	82.5	4.5	1.6	
	H4	1487.3	−31.4	4.8	0.3	342.5	150.5	43.9	96.2	4.0	1.6	
	H5	1496.3	−12.4	8.4	0.1	357.8	142.8	38.5	88.9	4.4	1.5	
FH	H6	2835.8	−10.3	3.1	0.0	391.6	141.2	36.0	80.5	4.8	1.4	mixed assemblage algae, Porifera, Pennatulacea, Bivalvia, Ascidiacea, Nemertea
	H7	2665.1	−38.4	3.3	0.2	377.5	131.6	34.2	82.9	4.7	1.4	
	H8	3135.6	−35.3	3.6	0.1	409.6	125.1	30.3	73.6	5.2	1.3	
	H9	3077.3	−11.2	2.8	0.0	224.4	119.8	25.5	67.0	5.8	1.3	
MH	H10	3818.8	−112.8	1.7	0.1	382.5	120.6	28.0	71.8	5.3	1.4	

lithogenic suspended matter from glacier

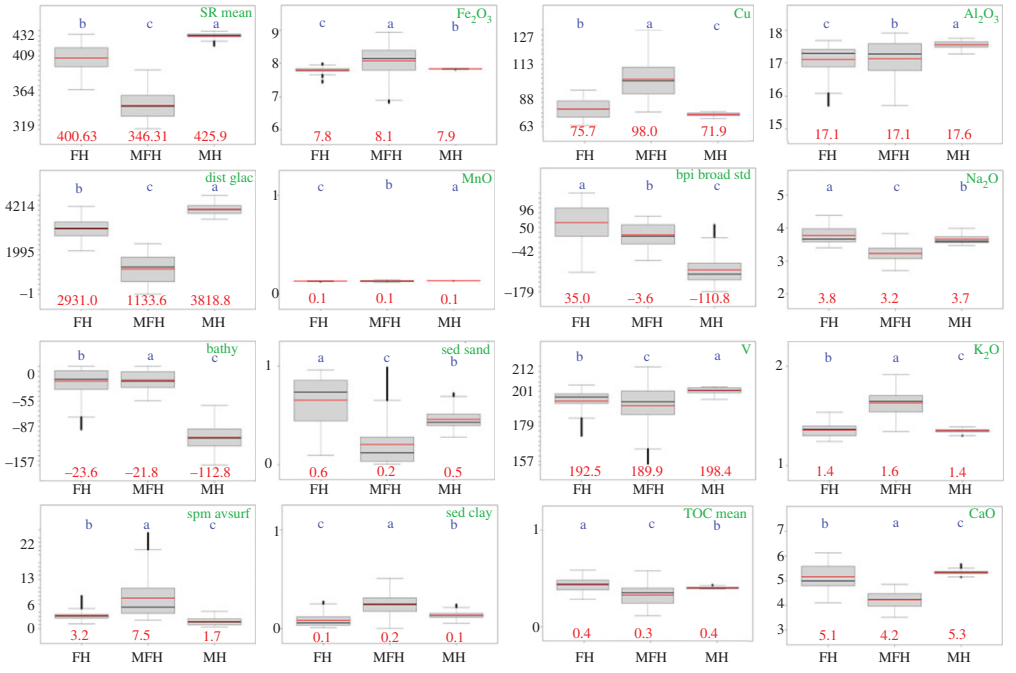

Figure 6. Data distribution (skewness, spread and outlying points) of selected variables within the habitats according to the probability of mean differences (ANOVA, α-level 0.5) and pair-wise confidence level from Tukey's HSD (95%). Black and red lines are the median and mean values. Red numbers are the mean values; the order of the blue letters represents the degree of similarity between the habitats. Habitats assigned to the same letter would not be significantly different. For the location of the habitats, refer to figure 4*d*. For variable units, refer to table 1.

the region, the extent to which different inshore systems respond to this change is not uniform. Rapidly changing systems, such as the smaller ice caps of the South Shetland Islands, are early indicators for processes predicted to affect the larger ice masses on the mainland WAP in the future. Spatial analysis of a multitude of variables is required to understand how glacial retreat affects local inshore and regional offshore ecosystems. The statistical ecosystem models applied here are valuable tools that exploit multi-layered datasets, combining diverse parameters of abiotic and biotic factors (descriptors), in order to classify different states of system change and to delineate the best environmental descriptors characterizing 'transitional' or 'final states' of system change. In the present paper, we used the multi-layered dataset from Potter Cove to characterize the transitional state of meltwater-influenced habitats (MFH) and distinguish them from a final state of now exclusively marine habitats (MH) in Potter Cove. These benthic habitats have passed through the same melt-influenced state within the recent 10 000 years [54], during which the frontline of the Fourcade Glacier retreated, albeit discontinuously, towards its present position on land [7]. More than only describing the momentary spatial compartmentalization of different meltwater and marine clusters or zones in Potter Cove, our analysis reveals a set of environmental variables that can be used to distinguish the recently melt-influenced zones from mature marine habitats in the inshore systems of KGI, and potentially the whole South Shetland archipelago. Most of the variables are easy to measure and are correlated (electronic supplementary material, appendix S2) with shallow bathymetry and the presence of geochemical indicators for lithogenic creek discharge and subglacial sediments. They are therefore positioned in the upper part of the ranking list and include glacier distance to habitats, bathymetry and BPI [36], in addition to selected geochemical elements related to the surrounding terrestrial host rock (figure 5*c*).

(a) Topological, sedimentological and biogeochemical interpretation of factorial cluster differentiation

A minimum number of 10 sub-habitats were required to identify the maximum extent of meltwater influence in Potter Cove. This was derived from non-hierarchical *k*-means clustering of 42 abiotic variables (see figure 3*a* and table 1). For the full list of statistical mean values of environmental variables comparing H1–H10, refer to the electronic supplementary material, appendix S1; table S3. Of these 10 clusters, five sub-habitats (clusters H1–H5) can be combined to form the overall zone of MFHs. MFHs are strongly discriminated by low Sr (346 mg kg^{-1}) and CaO (4.2 wt%) values from FHs and the surrounding terrestrial host rocks. MFHs have a maximum glacier distance of about 2270 m, and their seabed morphology is characterized by a positive BPI from glacial depressions that function as catchment areas for soft sediments, explaining the clay-dominated sediment texture of the MFHs. MFH sediments further contain relatively low TOC concentrations (figure 6) due to sparse colonization by macroalgae in these newly ice-free areas [23,55]. Furthermore, high sediment accumulation rates closer to the glacier lead to further dilution of the low organic fraction contained in these sediments.

Four of the 10 clusters were combined to form the FH (H6–H9, mean water depth −24 m), which occupies a similar water depth to the MFH (mean −22 m). The FH is more distant from the glacier (mean/max distance 2930 m), with reduced meltwater influence indicated by higher Sr (mean 400 mg kg^{-1}) and CaO (mean 5.1 wt%) concentrations, as well as a higher proportion of sand (mean *ca* 65%) in surface sediments. The strictly MH far from glacial influence (cluster 10) is clearly separated from the FH and MFH by bathymetry (mean water depth −112 m, figure 6). Some factors decrease gradually between the glacier front (MFH) and MHs, such as the wave energy in shallow water depths [38]. Additionally, fine sediments and clay undergo progressive washout by resuspension as surface sediments 'mature' in areas more remote from the glacier (table 3).

An incremental depletion of CaO associated with a slight depletion of Sr in sediments from MFH to MH (table 3) is one of the main distinguishing criteria in our study. It should be noted that the mean Sr (346 mg kg^{-1}) and CaO concentrations (4.2 wt%) in MFH sediments are lower than would be expected based on geochemical data of local bedrock (Ca: 7.1–9.3 wt%, Sr: 527–609 mg kg^{-1} [56–59]). A similar phenomenon was observed by Lee *et al*. [53], who investigated soils and bedrock on the nearby Barton Peninsula. These authors proposed lower CaO and Sr concentrations in soils compared with the underlying bedrock to be the result of plagioclase alteration. They suggested that CaO depletion in feldspar is caused by chelating agents excreted by lichens covering local soils and rock debris [53]. It is therefore quite likely that lower mean Sr and CaO concentrations found in MFH sediments are the result of biochemical weathering of soils and terrestrial sediments, mainly from Potter Peninsula, due to earlier deglaciation than Barton Peninsula [54].

The combination of low TOC content and high concentrations of iron and manganese in sediments and pore water has been reported in several recent studies in coastal Arctic and Antarctic regions [25,60]. Elevated concentrations of Mn and Fe in pore water close to the glacier front [25] indicate that dissimilatory metal reduction is the main driver of organic matter degradation in these sediments. While only a small amount of Fe and Mn released by these sediments will be complexed in the water column, the major part of these transition metals is re-oxidized and re-deposited, explaining the relative increase in sedimentary Fe and Mn in the sediment surface of the MFH [26]. By contrast, in FH areas where TOC concentrations are higher (figure 6, only in the central deeper parts), organic matter oxidation is predominantly based on sulfate reduction rather than on Fe reduction [25], so that Fe accumulation in surface sediments is not enhanced.

The habitat mapping approach introduced in this paper is mainly data driven and does not directly depend on a mechanistic understanding of the underlying geochemical processes. It is mostly automatic and allows the classification to be refined at certain stages, based on visual inspections of the analytical results (e.g. decision-making for the best cluster number). All in all,

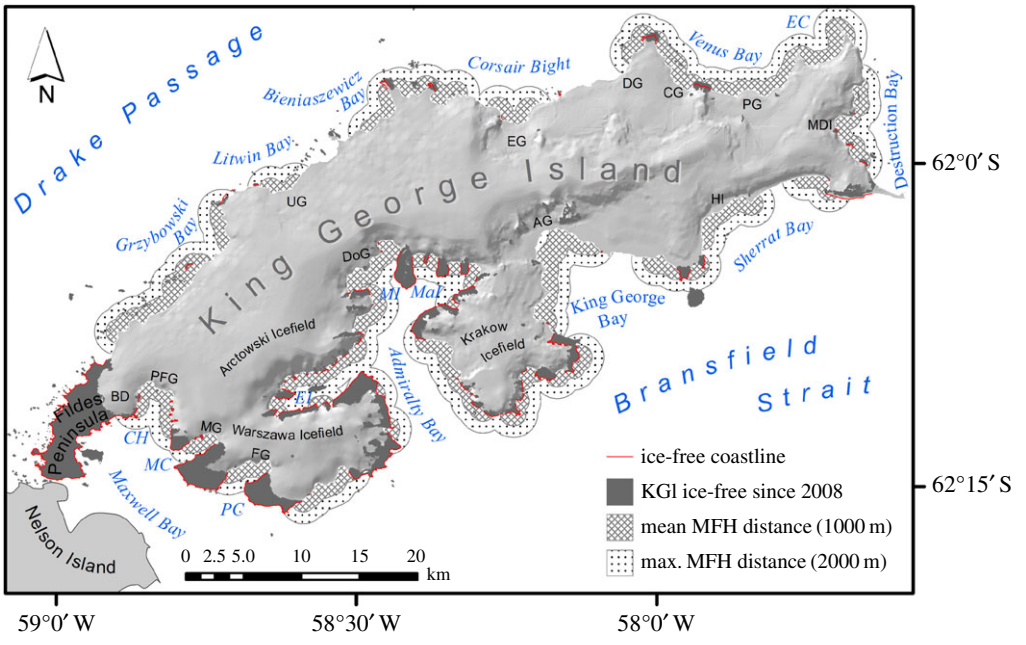

Figure 7. Properties of the KGI coast assigned to the inferred MFH are the mean and maximum distance to the glacier experienced at Potter Cove as well as glaciers adjacent to the coast and the coast shape (fjords or bays). AG, Anna Glacier; BD, Bellinghausen Dome; CG, Crystal Glacier; DG, Drake Glacier; DoG, Domeyko Glacier; EG, Eldred Glacier; FG, Fourcade Glacier; HI, Hektors Icefall; MDI, Moby Dick Icefall; MG, Moczydlowski Glacier; PFG, Polar Friendship Glacier; PG, Poetry Glacier; UG, Sher Glacier; CH, Collins Harbour; EC, Esmerald Cove; MC, Marian Cove; PC, Potter Cove; EI, Ezcurra Inlet; Mal, Mackellar Inlet; MI, Martel Inlet. (Data derived from Rückamp *et al*. [7].)

our study is a purely statistical approach to the data, which has both strengths and weaknesses. However, the results presented in this study are repeatable and with a resolution and precision limited only by the data input [61]. In the optimal case, the results from a cluster analysis can be interpreted based on the state of scientific knowledge with respect to biogeochemistry and ecology (see above).

(b) Missing information that would add to the analytical output

The cluster analytical results could be improved by including hydrodynamics and wind data for the Potter Cove area. Tides, meltwater run-off and ice scouring influence mixing intensity and hence the resuspension and deposition patterns of lithogenic SPM. These processes cause fractionation of sediments and minerals and decrease benthic biodiversity [55], respectively. Including the cyclonic surface circulation pattern into the present analysis would facilitate the interpretation of biochemical patterns and help to explain differences between southern and northern clusters within the three fjord habitat zones (MFH, FH, MH). Analysis of the mineralogical composition on the Barton and Potter Peninsulas (N.T. Manograsso-Czalbowski 2017, unpublished data and personal communication) needs to be combined with a geochemical element analysis in surface sediments on both sides of the cove for a better understanding of lithogenic fluxes and provenance (clay mineral composition) compared with the distribution of markers for biogenic productivity (carbonate, biogenic opal, TOC).

(c) Upscaling the ecological consequences of glacier melt

Rapid glacier retreat in Potter Cove has caused shifts in benthic assemblages [27] that can be associated with the identified meltwater habitats (table 3). The use of data from recent

sediments in the upper 5 cm surface layer, equalling approximately 5–10 years of sediment deposition, implies that we can link the resulting habitat patterns to the most recent ecological shifts occurring in the cove [10,26,28,29,62]. The next step would then be to quantify the extent of coastal areas affected by meltwater input and sedimentation, potentially resulting in similar effects on marine communities. Here, we estimate for the first time the impact radius of glacial discharge by defining the extent of the MFH for a model cove on KGI. Rückamp *et al*. [7] published the retreating tidewater glacier front lines for KGI derived from satellite imagery between 1956 and 2008. From these lines, we calculated the amount of newly ice-free marine areas to approx. 75 km^2 along KGI. The share of Potter Cove amounts to an area of 1.4 km^2. With this knowledge, a first approximation of the total extent of meltwater-impacted habitats along KGI can be provided. This estimate is derived for 200 km of coastline currently occupied by tidewater glaciers and located inside the geomorphological features of inshore fjords and bays (figure 7) of the island (approx. 40% of the overall ice-covered island coastline of 457 km). To these manually identified sections of the KGI coastline, a Euclidean buffering of 1000 m and 2000 m (mean and maximum MFH distance in Potter Cove) MFH was applied and projected in UTM21 coordinates in ArcGIS 10.4.1 (ESRI). The resulting estimation amounts to between 200 km^2 (conservative approximation) and 400 km^2 (maximum extension) of present MFH extension.

This paper is the first algorithmic approach to approximate meltwater-impacted coastal inshore areas based on abiotic data from an ecosystem study in a 'model cove'. It reveals the extent to which coastal inshore areas at KGI are currently impacted and can further be applied more widely on the WAP [3] to approximate the extent of potential future melt-impacted habitats (figure 7). These terrestrial marine transition areas are of major importance for coastal biogeochemistry and marine biodiversity and the rapid changes happening here are bound to affect larger shelf and open ocean areas.

Data accessibility. The datasets supporting this article have been uploaded as part of the electronic supplementary material, appendices S1 and S2, and are accessible from the data archive Pangaea (https://doi.pangaea.de/10.1594/PANGAEA.856971) [37].

Authors' contributions. K.J. conceived of and designed the study, performed the data analysis and drafted the manuscript. H.P. performed data analysis and R programming. P.M. carried out sediment sampling, geochemical analyses and discussed geochemical datasets. F.S. performed data management and data analysis. L.W. performed data management and R programming. G.K. commented on the study and on the manuscript. M.H.B. carried out data glaciological data acquisition. D.A. contributed to the design of the study and the data acquisition. All authors read and approved the manuscript and met all the following criteria: (i) substantial contributions to conception and design, or acquisition of data, or analysis and interpretation of data; (ii) drafting the article or revising it critically for important intellectual content; and (iii) final approval of the version to be published.

Competing interests. We declare we have no competing interests.

Funding. The research was funded by grants JE 680/1-1 and BR 775/25-1 from the German Research Foundation (DFG) in the SSP 1158 Priority Program Antarctic Research, DFG grant BR 2105/13-1 and the EU research network IMCONet funded by the Marie Curie Action IRSES (FP7 IRSES, action no. 318718). Source of funding for each author is as follows: AWI, DFG SSP 1158 grant JE 680/1-1; Marie Curie Action FP 7 IRSES (action no. 318718) (to K.J.); AWI (to H.P. and L.W.); ICBM, DFG SSP 1158 grant BR 775/25-1 (to P.M.); AWI, Marie Curie Action FP 7 IRSES (action no. 318718) (to F.S., G.K. and D.A.); DFG grant BR 2105/13-1 (to M.H.B.).

Acknowledgement. The work has been performed based on data collected at Carlini Station/Dallmann Laboratory, within the framework of the scientific collaboration existing between Instituto Antartico Argentino/Direccion Nacional del Antartico and the Alfred Wegener Institute, Helmholtz Centre for Polar and Marine Research.

References

1. Turner J *et al.* 2013 Antarctic climate change and the environment: an update. *Polar Rec.* **50**, 237–259. (doi:10.1017/S0032247413000296)

2. Stammerjohn S, Massom R, Rind D, Martinson D. 2012 Regions of rapid sea ice change: an inter-hemispheric seasonal comparison. *Geophys. Res. Lett.* **39**, L06501. (doi:10.1029/2012GL050874)
3. Cook AJ, Holland PR, Meredith MP, Murray T, Luckman A, Vaughan DG. 2016 Ocean forcing of glacier retreat in the western Antarctic Peninsula. *Science* **353**, 283–286. (doi:10.1126/science.aae0017)
4. Bers AV, Momo F, Schloss IR, Abele D. 2012 Analysis of trends and sudden changes in long-term environmental data from King George Island (Antarctica): relationships between global climatic oscillations and local system response. *Clim. Change.* **116**, 789–803. (doi:10.1007/s10584-012-0523-4)
5. Meredith MP, Falk U, Bers AV, Mackensen A, Schloss IR, Ruiz Barlett E. 2018 Anatomy of a glacial meltwater discharge event in an Antarctic cove. *Phil. Trans. R. Soc. A* **376**, 20170163. (doi:10.1098/rsta.2017.0163)
6. Osmanoğlu B, Braun M, Hock R, Navarro FJ. 2013 Surface velocity and ice discharge of the ice cap on King George Island, Antarctica. *Ann. Glaciol.* **54**, 111–119. (doi:10.3189/2013AoG63A517)
7. Rückamp M, Braun M, Suckro S, Blindow N. 2011 Observed glacial changes on the King George Island ice cap, Antarctica, in the last decade. *Glob. Planet. Change.* **79**, 99–109. (doi:10.1016/j.gloplacha.2011.06.009)
8. Barnes DK. 2017 Polar zoobenthos blue carbon storage increases with sea ice losses, because across-shelf growth gains from longer algal blooms outweigh ice scour mortality in the shallows. *Glob. Change Biol.* **23**, 5083–5091. (doi:10.1111/gcb.13772)
9. Ducklow H *et al.* 2013 West Antarctic Peninsula: an ice-dependent coastal marine ecosystem in transition. *Oceanography* **26**, 190–203. (doi:10.5670/oceanog.2013.62)
10. Slemmons KE, Saros JE, Simon K. 2013 The influence of glacial meltwater on alpine aquatic ecosystems: a review. *Environ. Sci. Process. Impacts.* **15**, 1794–1806. (doi:10.1039/c3em00243h)
11. Steinberg D, Martinson D, Costa D. 2012 Two decades of pelagic ecology of the Western Antarctic Peninsula. *Oceanography* **25**, 56–67. (doi:10.5670/oceanog.2012.75)
12. Convey P *et al.* 2014 The spatial structure of Antarctic biodiversity. *Ecol. Monogr.* **84**, 203–244. (doi:10.1890/12-2216.1)
13. Lagger C, Nime M, Torre L, Servetto N, Tatián M, Sahade R. 2017 Climate change, glacier retreat and a new ice-free island offer new insights on Antarctic benthic responses. *Ecography* **41**(4), 579–591. (doi:10.1111/ecog.03018)
14. Philipp EER, Husmann G, Abele D. 2011 The impact of sediment deposition and iceberg scour on the Antarctic soft shell clam *Laternula elliptica* at King George Island, Antarctica. *Antarct. Sci.* **23**, 127–138. (doi:10.1017/S0954102010000970)
15. Post AL, Lavoie C, Domack EW, Leventer A, Shevenell A, Fraser AD. 2017 Environmental drivers of benthic communities and habitat heterogeneity on an East Antarctic shelf. *Antarct. Sci.* **29**, 17–32. (doi:10.1017/S0954102016000468)
16. Sahade R, Tatián M, Kowalke J, Kühne S, Esnal GB. 1998 Benthic faunal associations on soft substrates at Potter Cove, King George Island, Antarctica. *Polar Biol.* **19**, 85–91. (doi:10.1007/s003000050218)
17. Seefeldt MA, Weigand AM, Havermans C, Moreira E, Held C. 2017 Fishing for scavengers: an integrated study to amphipod (Crustacea: Lysianassoidea) diversity of Potter Cove (South Shetland Islands, Antarctica). *Mar. Biodiver.* (doi:10.1007/s12526-017-0737-9)
18. Tatian M, Sahade RJ, Doucet ME, Esnal GB. 2004 Ascidians (Tunicata, Ascidiacea) of Potter Cove, South Shetland Islands, Antarctica. *Antarct. Sci.* **10**, 147–152. (doi:10.1017/S0954102098000194)
19. Pecl GT *et al.* 2017 Biodiversity redistribution under climate change: impacts on ecosystems and human well-being. *Science* **355**, 1–9. (doi:10.1126/science.aai9214)
20. Poloczanska ES *et al.* 2016 Responses of marine organisms to climate change across oceans. *Front. Mar. Sci.* **3**, e62. (doi:10.3389/fmars.2016.00062)
21. Jerosch K *et al.* Submitted. Habitat modeling as a predictive tool for analyzing spatial shifts in Antarctic benthic communities due to global climate change.
22. Schloss IR, Abele D, Moreau S, Demers S, Bers AV, González O, Ferreyra GA. 2012 Response of phytoplankton dynamics to 19-year (1991–2009) climate trends in Potter Cove (Antarctica). *J. Mar. Sys.* **92**, 53–66. (doi:10.1016/j.jmarsys.2011.10.006)

23. Monien D, Monien P, Brünjes R, Widmer T, Kappenberg A, Silva BAA, Schnetger B, Brumsack H-J. 2017 Meltwater as a source of potentially bioavailable iron to Antarctica waters. *Antarct. Sci.* **29**, 277–291. (doi:10.1017/S095410201600064X)
24. Silva BAA, Falk U, Pölcher P. 2018 A simplified method to estimate the runoff in periglacial creeks. Case study: King George Islands, Antarctic Peninsula. *Phil. Trans. R. Soc. A* **376**, 20170166. (doi:10.1098/rsta.2017.0166)
25. Monien P *et al.* 2014 Redox conditions and trace metal cycling in coastal sediments from the maritime Antarctic. *Geochim. Cosmochim. Acta.* **141**, 26–44. (doi:10.1016/j.gca.2014.06.003)
26. Poigner H, Monien P, Monien D, Kriews M, Brumsack H-J, Wilhelms-Dick D, Abele D. 2013 Influence of the porewater geochemistry on Fe and Mn assimilation in Laternula elliptica at King George Island (Antarctica). *Estuar. Coast. Shelf Sci.* **135**, 285–295. (doi:10.1016/j.ecss.2013.10.027)
27. Sahade R *et al.* 2015 Climate change and glacier retreat drive shifts in an Antarctic benthic ecosystem. *Sci. Adv.* **1**, e1500050. (doi:10.1126/sciadv.1500050)
28. Torre L, Tabares PCC, Momo F, Meyer JFCA, Sahade R. 2017 Climate change effects on Antarctic benthos: a spatially explicit model approach. *Clim. Change.* **141**, 733–746. (doi:10.1007/s10584-017-1915-2)
29. Brey T, Voigt M, Jenkins K, Ahn I-Y. 2011 The bivalve Laternula elliptica at King George Island — a biological recorder of climate forcing in the West Antarctic Peninsula region. *J. Mar. Sys.* **88**, 542–552. (doi:10.1016/j.jmarsys.2011.07.004)
30. Torre L, Abele D, Lagger C, Momo F, Sahade R. 2014 When shape matters: strategies of different Antarctic ascidians morphotypes to deal with sedimentation. *Mar. Environ. Res.* **99**, 179–187. (doi:10.1016/j.marenvres.2014.05.014)
31. Pasotti F, Manini E, Giovannelli D, Wölfl A-C, Monien D, Verleyen E, Braeckman U, Abele D, Vanreusel A. 2015 Antarctic shallow water benthos in an area of recent rapid glacier retreat. *Mar. Ecol.* **36**, 716–733. (doi:10.1111/maec.12179)
32. Quartino ML, Deregibus D, Campana GL, Latorre GE, Momo FR. 2013 Evidence of macroalgal colonization on newly ice-free areas following glacial retreat in Potter Cove (South Shetland Islands), Antarctica. *PLoS ONE* **8**, e58223. (doi:10.1371/journal.pone.0058223)
33. Lindhorst S, Schutter I. 2014 Polar gravel beach-ridge systems: sedimentary architecture, genesis, and implications for climate reconstructions (South Shetland Islands/Western Antarctic Peninsula). *Geomorphology* **221**, 187–203. (doi:10.1016/j.geomorph.2014.06.013)
34. Wölfl A-C, Wittenberg N, Feldens P, Hass HC, Betzler C, Kuhn G. 2016 Submarine landforms related to glacier retreat in a shallow Antarctic fjord. *Antarct. Sci.* **28**, 475–486. (doi:10.1017/S0954102016000262)
35. Wölfl A-C, Lim CH, Hass HC, Lindhorst S, Tosonotto G, Lettmann KA, Kuhn G, Wolff JO, Abele D. 2014 Distribution and characteristics of marine habitats in a subpolar bay based on hydroacoustics and bed shear stress estimates—Potter Cove, King George Island, Antarctica. *Geo-Mar. Lett.* **34**, 435–446. (doi:10.1007/s00367-014-0375-1)
36. Weiss AD. 2001 Topographic positions and landforms analysis. In *Proc. of the 21st Annu. ESRI Int. User Conf., San Diego, CA, 9–13 July 2001*. See http://www.jennessent.com/downloads/TPI-poster-TNC_18x22.pdf.
37. Jerosch K, Scharf FK. 2015 High resolution bathymetric compilation for Potter Cove, WAP, Antarctica, with links to data in ArcGIS format. *Pangaea*. (doi:10.1594/PANGAEA.853593)
38. Lim CH, Lettmann K, Wolff J-O. 2013 Numerical study on wave dynamics and wave-induced bed erosion characteristics in Potter Cove, Antarctica. *Ocean Dyn.* **63**, 1151–1174. (doi:10.1007/s10236-013-0651-z)
39. Iampietro P, Kvitek R (eds). 2002 Quantitative seafloor habitat classification using GIS terrain analysis: effects of data density, resolution, and scale. In *Proc. of the 22nd Annu. ESRI Int. User Conf., San Diego, CA, 8–12 July 2001*. ESRI.
40. Jerosch K, Kuhn G, Krajnik I, Scharf FK, Dorschel B. 2015 A geomorphological seabed classification for the Weddell Sea, Antarctica. *Mar. Geophys. Res.* **37**, 127–141. (doi:10.1007/s11001-015-9256-x)
41. R Core Team. 2017 *R: A language and environment for statistical computing*. Vienna, Austria: R Foundation for Statistical Computing. See http://www.R-project.org/.
42. Kaufman L, Rousseeuw PJ. 2009 *Finding groups in data: an introduction to cluster analysis*, 3rd edn, p. 349. Wiley Series in Probability and Statistics. Hoboken, NJ: John Wiley & Sons.

43. Greenacre M, Primicerio R. 2014 *Multivariate analysis of ecological data*. Bilbao, Spain: Fundación BBVA.
44. Charrad M, Ghazzali N, Boiteau V, Niknafs A. 2014 NbClust: An R package for determining the relevant number of clusters in a data set. *J. Stat. Softw.* **61**, 1–36. (doi:10.18637/jss.v061.i06)
45. Tibshirani R, Walther G, Hastie T. 2001 Estimating the number of data clusters via the Gap statistic. *J. R. Stat. Soc. B* **63**, 411–423. (doi:10.1111/1467-9868.00293)
46. Zhao Q, Fränti P. 2014 WB-index: a sum-of-squares based index for cluster validity. *Data Know. Eng.* **92**, 77–89. (doi:10.1016/j.datak.2014.07.008)
47. Aitchison J. 1986 *The statistical analysis of compositional data*. London, UK: Chapman & Hall.
48. Dormann CF *et al.* 2013 Collinearity: a review of methods to deal with it and a simulation study evaluating their performance. *Ecography* **36**, 27–46. (doi:10.1111/j.1600-0587.2012.07348.x)
49. Drukker DM. 2003 Testing for serial correlation in linear panel-data models. *Stat. J.* **3**, 168–177.
50. Hotelling H. 1936 Relations between two sets of variates. *Biometrika* **28**, 321–377. (doi:10.1093/biomet/28.3-4.321)
51. Härdle WK, Simar L. 2015 Canonical correlation analysis. In *Applied multivariate statistical analysis*, pp. 443–454. Berlin, Germany: Springer.
52. Härdle W, Simar L. 2007 Canonical correlation analysis. In *Applied multivariate statistical analysis*, pp. 321–330. Berlin, Germany: Springer.
53. Lee YI, Lim HS, Yoon HI. 2004 Geochemistry of soils of King George Island, South Shetland Islands, West Antarctica: implications for pedogenesis in cold polar regions. *Geochim. Cosmochim. Acta.* **68**, 4319–4333. (doi:10.1016/j.gca.2004.01.020)
54. Simms AR, Milliken KT, Anderson JB, Wellner JS. 2011 The marine record of deglaciation of the South Shetland Islands, Antarctica since the Last Glacial Maximum. *Quat. Sci. Rev.* **30**, 1583–1601. (doi:10.1016/j.quascirev.2011.03.018)
55. Deregibus D, Quartino ML, Zacher K, Campana GL, Barnes DKA. 2017 Understanding the link between sea ice, ice scour and Antarctic benthic biodiversity—the need for cross-station and international collaboration. *Polar Rec.* **53**, 143–152. (doi:10.1017/S0032247416000875)
56. Kraus S, Poblete F, Arriagada C. 2010 Dike systems and their volcanic host rocks on King George Island, Antarctica: implications on the geodynamic history based on a multidisciplinary approach. *Tectonophysics* **495**, 269–297. (doi:10.1016/j.tecto.2010.09.035)
57. Machado A *et al.* 2005 Geochemistry constraints of Mesozoic–Cenozoic calc-alkaline magmatism in the South Shetland arc, Antarctica. *J. South Amer. Earth Sci.* **18**, 407–425. (doi:10.1016/j.jsames.2004.11.011)
58. Smellie JL, Pankhurst RJ, Thomson MRA, Davies RES. 1984 The geology of the South Shetland Islands: VI. Stratigraphy, geochemistry and evolution. *Br. Antarct. Sur. Sci. Rep.* **87**, 1–86.
59. Yeo JP, Lee JI, Do Hur S, Choi B-G. 2004 Geochemistry of volcanic rocks in Barton and Weaver peninsulas, King George Island, Antarctica: implications for arc maturity and correlation with fossilized volcanic centers. *Geosci. J.* **8**, 11. (doi:10.1007/BF02910275)
60. Wehrmann LM, Formolo MJ, Owens JD, Raiswell R, Ferdelman TG, Riedinger N, Lyons TW. 2014 Iron and manganese speciation and cycling in glacially influenced high-latitude fjord sediments (West Spitsbergen, Svalbard): evidence for a benthic recycling-transport mechanism. *Geochim. Cosmochim. Acta.* **141**, 628–655. (doi:10.1016/j.gca.2014.06.007)
61. Wright DJ, Heyman WD. 2008 Introduction to the special issue: marine and coastal GIS for geomorphology, habitat mapping, and marine reserves. *Mar. Geodesy* **31**, 223–230. (doi:10.1080/01490410802466306)
62. Deregibus D, Quartino ML, Campana GL, Momo FR, Wiencke C, Zacher K. 2016 Photosynthetic light requirements and vertical distribution of macroalgae in newly ice-free areas in Potter Cove, South Shetland Islands, Antarctica. *Polar Biol.* **39**, 153–166. (doi:10.1007/s00300-015-1679-y)